

Cooperative Jahn–Teller Interactions in Dynamic Copper(II) Complexes. Temperature Dependence of the Crystal Structure and EPR Spectrum of Deuterated Ammonium Copper(II) Sulfate Hexahydrate

Michael A. Hitchman,^{*,†} Wim Maaskant,[‡] Jaco van der Plas,[‡] Charles J. Simmons,[§] and Horst Stratemeier[†]

Contribution from the Chemistry Department, University of Tasmania, Box 252-75, Hobart, Tasmania 7001, Australia, Gorlaeus Laboratories, Leiden Institute of Chemistry, University of Leiden, P.O. Box 9502, 2300 RA Leiden, The Netherlands, and Mathematics and Science Division, Brigham Young University—Hawaii, Laie, Hawaii 96762

Received May 26, 1998

Abstract: The crystal structure of the deuterated Tutton salt $(\text{ND}_4)_2[\text{Cu}(\text{D}_2\text{O})_6](\text{SO}_4)_2$ determined by X-ray diffraction at several temperatures between 100 and 321 K is reported. The intermediate and longest Cu–O bond lengths of the Jahn–Teller distorted octahedral $\text{Cu}(\text{D}_2\text{O})_6^{2+}$ ion progressively converge as the temperature is raised above ~ 200 K, and this is accompanied by a partial rotation of the ammonium and sulfate groups. The g -values derived from the EPR spectrum of the compound exhibit similar behavior, as do those of $\sim 1\%$ Cu^{2+} doped into the isomorphous zinc(II) compound. The temperature dependence of the g -values of Cu^{2+} -doped $(\text{ND}_4)_2[\text{Zn}(\text{D}_2\text{O})_6](\text{SO}_4)_2$ may be interpreted satisfactorily by a model which assumes a Boltzmann thermal distribution between two energy states which differ solely in the orientation of the $\text{Cu}(\text{D}_2\text{O})_6^{2+}$ ion in the lattice. However, such a model does not satisfactorily explain the behavior of pure $(\text{ND}_4)_2[\text{Cu}(\text{D}_2\text{O})_6](\text{SO}_4)_2$, and it is suggested that this is due to cooperative interactions. A new model, in which the probable energy state of each complex is estimated after taking into account the likely orientations of its neighbors in the lattice, is described. Application of this model suggests that the thermal behavior is dominated by the cooperative interactions between complexes, these being transmitted via the hydrogen-bonding network. Comparisons are drawn with the cooperative interactions observed in more strongly coupled Jahn–Teller systems and in compounds for which the structural changes are associated with equilibria between two spin states.

Introduction

The stereochemistry and spectroscopic properties of Cu^{2+} complexes are generally interpreted in terms of Jahn–Teller coupling,¹ this being termed “dynamic” when the geometry and electronic structure change as a function of temperature. Interest in this area has recently been stimulated by the suggestion that dynamic Jahn–Teller coupling may be involved in the mechanism underlying the behavior of high-temperature superconductors.² Moreover, the electron paramagnetic resonance (EPR) spectra of certain copper “blue” proteins vary with temperature, and it has been suggested that this is due to dynamic vibronic coupling effects.³ Early reports of such behavior focused on systems where a complex is essentially localized in one state, with a higher state being admixed into this ground state by a vibronic coupling mechanism analogous to that which provides the intensity in Laporte-forbidden electronic transitions.^{4,5} Here, the dynamic effects result from the thermal population of upper

levels of the vibrational states acting to mix in the higher electronic state. Such behavior is rather rare. More commonly, dynamic effects are associated with a warped ground-state potential energy surface. In this case, the warping is caused by higher-order effects and interactions with the surrounding lattice, and the dynamic behavior is caused by the fact that some of the resulting vibronic levels correspond to different orientations of the complex in the crystal. When these vibronic levels are close in energy, their population depends on temperature, so that the average geometry and electronic structure of the complex is temperature dependent. Experimentally, the geometric changes are normally observed by X-ray or neutron diffraction,⁶ while the electronic wave functions are studied by EPR spectroscopy.⁷

A theoretical model was recently developed to interpret the properties of “fluxional” copper(II) complexes of this kind.⁸ Initially, this was used to interpret the temperature-dependent g -values of six-coordinate Cu^{2+} complexes in terms of second-order Jahn–Teller coupling and the influence of low-symmetry components of the ligand field,⁹ with the model subsequently being extended to include the concomitant changes in the

[†] University of Tasmania.

[‡] University of Leiden.

[§] Brigham Young University—Hawaii.

(1) Hathaway, B. J. *Struct. Bonding* **1984**, 57, 55.

(2) Markiewicz, R. S. *J. Phys. Chem. Solids* **1995**, 15, 1637. Fil, D. V.; Tokar, O. I.; Shelankov, A. L.; Weber, W. *Phys. Rev. B* **1992**, 45, 5633 and references therein.

(3) Bacci, M. *New J. Chem.* **1993**, 17, 67.

(4) O'Brien, M. C. M. *Proc. R. Soc.* **1964**, 281A, 323.

(5) Riley, M. J.; Hitchman, M. A. *Chem. Phys.* **1986**, 102, 11.

(6) Simmons, C. J. *New J. Chem.* **1993**, 17, 77 and references therein.

(7) Silver, B. L.; Getz, D. *J. Chem. Phys.* **1974**, 61, 638.

(8) Hitchman, M. A. *Comments Inorg. Chem.* **1994**, 15, 197.

(9) Riley, M. J.; Hitchman, M. A.; Wan Mohammed, A. *J. Chem. Phys.* **1987**, 87, 3766.

metal–ligand bond lengths.¹⁰ The behavior of the complexes formed by “doping” Cu²⁺ into various host lattices was interpreted successfully using this approach,^{9–12} and the model was also applied to a range of pure copper(II) complexes exhibiting dynamic behavior.^{13–16} In some cases, a distribution of the different structural forms remained even after cooling to 4 K, making it hard to determine the nature of the complexes unambiguously.^{15,16} Here, measurement of the extended X-ray absorption fine structure (EXAFS) proved a useful method of confirming the geometries of the complexes at the local level.^{16,17}

Particularly interesting dynamic behavior is observed for the copper(II) Tutton salts, of general formula (cation)₂[Cu(H₂O)₆](SO₄)₂. The fluxional behavior of the octahedral Cu(H₂O)₆²⁺ group created when Cu²⁺ is doped into the zinc(II) Tutton salts formed with a range of cations has been studied by EPR spectroscopy,^{7,9,18,19} and similar behavior has been reported for undiluted (NH₄)₂[Cu(H₂O)₆](SO₄)₂.^{20,21} The ammonium copper(II) Tutton salt is unusual because upon deuteration, although the crystallographic space group is the same, the long axis of the Jahn–Teller distorted Cu(D₂O)₆²⁺ complex occurs to a different pair of water molecules from that in the hydrogenous salt.²² Moreover, upon raising the pressure from 1 bar to 1.5 kbar at room temperature and cooling to 15 K, the deuterated compound adopts a structure analogous to that of the hydrogenous compound,²³ the first known example of such a pressure-dependent Jahn–Teller “switch”. For both the hydrogenous and deuterated salts, a dynamic equilibrium between the structural forms occurs at room temperature,²⁴ and the latter exhibits a hysteresis above ambient pressure.²⁵

To a first approximation, the variation of the *g*-values of (NH₄)₂[Cu(H₂O)₆](SO₄)₂ over a limited temperature range obeys a simple model which assumes a Boltzmann distribution over two energy states, each corresponding to a different orientation of the Cu(H₂O)₆²⁺ ion in the crystal lattice.²⁰ However, a more detailed study found significant deviations from this simple model at higher temperatures, and it has been suggested that

(10) Bebedorf, J.; Bürgi, H.-B.; Gamp, E.; Hitchman, M. A.; Murphy, A.; Reinen, D.; Riley, M. J.; Stratemeier, H. *Inorg. Chem.* **1996**, *35*, 7419.

(11) Riley, M. J.; Hitchman, M. A.; Reinen, D.; Steffen, G. *Inorg. Chem.* **1988**, *27*, 1924.

(12) Wagner, B.; Warda, S. A.; Hitchman, M. A.; Reinen, D. *Inorg. Chem.* **1996**, *35*, 3967.

(13) Headlam, H.; Hitchman, M. A.; Stratemeier, H.; Smits, J. M. M.; Beurskens, P. T.; de Boer, E.; Janssen, G.; Gatehouse, B. M.; Deacon, G. B.; Ward, G. N.; Riley, M. J.; Wang, D. *Inorg. Chem.* **1995**, *34*, 5516.

(14) Astley, T.; Headlam, H.; Hitchman, M. A.; Keene, F. R.; Pilbrow, J.; Stratemeier, H.; Tiekink, E.; Zhong, Y. C. *J. Chem. Soc., Dalton Trans.* **1995**, 3809.

(15) Tucker, D.; White, P. S.; Trojan, K. L.; Kirk, M. L.; Hatfield, W. E.; *Inorg. Chem.* **1991**, *30*, 823. Stratemeier, H.; Wagner, B.; Krausz, E. R.; Lindner, R.; Schmidtke, H.-H.; Pebler, J.; Hatfield, W. E.; ter Haar, L.; Reinen, D.; Hitchman, M. A. *Inorg. Chem.* **1994**, *33*, 2320.

(16) Astley, T.; Ellis, P. J.; Freeman, H.; Hitchman, M. A.; Keene, F. R.; Tiekink, E. R. T. *J. Chem. Soc., Dalton Trans.* **1995**, 595.

(17) Ellis, P. J.; Freeman, H.; Hitchman, M. A.; Reinen, D.; Wagner, B. *Inorg. Chem.* **1994**, *33*, 1249.

(18) Petrashen, V. E.; Yablokov, Yu V.; Davidovitch, R. L. *Phys. Status Solidi B* **1980**, *101*, 117.

(19) Misra, S. K.; Wang, Ch. *Phys. Rev. B* **1990**, *41*, 41; Rao, P.; Viswaneth, A. K.; Subramanian, S. *Spectrochim. Acta* **1992**, *48A*, 1745.

(20) Alcock, N. W.; Duggan, M.; Murray, A.; Tyagi, S.; Hathaway, B. J.; Hewat, A. *J. Chem. Soc., Dalton Trans.* **1984**, 7.

(21) Augustyniak, M. A.; Usachev, A. E.; Yablokov, Y. V. Private communication.

(22) Hathaway, B. J.; Hewat, A. W. *J. Solid State Chem.* **1984**, *51*, 364.

(23) Simmons, C. J.; Hitchman, M. A.; Stratemeier, H.; Schultz, A. J. *J. Am. Chem. Soc.* **1993**, *115*, 11304.

(24) Rauw, W.; Ahsbahs, H.; Hitchman, M. A.; Lukin, S.; Reinen, D.; Schultz, A.; Simmons, C. J.; Stratemeier, H. *Inorg. Chem.* **1996**, *35*, 1902.

(25) Schultz, A.; Hitchman, M. A.; Jorgensen, J. D.; Lukin, S.; Radaelli, P. G.; Simmons, C. J.; Stratemeier, H. *Inorg. Chem.* **1997**, *36*, 3383.

these might be due to cooperative interactions.²¹ The temperature dependence of the Cu–O bond lengths of the deuterated compound measured by powder neutron diffraction²² also reveals deviations from simple Boltzmann statistics, and here also it was proposed²³ that this could be caused by cooperative interactions between the complexes. To investigate this aspect properly, it is desirable to study the temperature dependence of both the EPR spectrum and the crystal structure of the same compound, since the two techniques provide complementary information.²⁵ We report here the EPR spectrum of deuterated ammonium copper sulfate hexahydrate recorded over a wide temperature range. Its crystal structure has also been redetermined more precisely by X-ray diffraction at a number of temperatures. To allow comparison with a system where cooperative interactions are absent, the EPR spectrum of Cu²⁺-doped (ND₄)₂[Zn(D₂O)₆](SO₄)₂ was also measured.

To interpret the data, the influence of cooperative interactions on the dynamic behavior is considered. The fact that cooperative Jahn–Teller interactions can have a significant effect on the crystal packing of copper(II) complexes is well established.^{26,27} Such interactions are responsible for the highly ordered packing arrangements often observed for Cu²⁺ compounds.^{28–30} However, previous studies of cooperative Jahn–Teller interactions have usually focused on compounds where the complexes are in close proximity and the cooperative interactions are therefore strong. The effect of temperature on such systems is normally different from that observed for the Tutton salts. Rather than each complex exhibiting a gradual change in apparent geometry within a unit cell which maintains its symmetry properties, a sharp, first-order phase transition occurs, involving a change in the space group to a new, ordered packing arrangement of the complexes. In these strongly coupled systems, the cooperative Jahn–Teller interactions are conventionally treated by means of parametrization schemes which refer to the whole ensemble of molecules in the lattice.^{26,31}

A rather different approach has been used in the present work. In the Tutton salts, the ligand molecules of neighboring complexes are not in direct contact. Rather, they are interconnected by a hydrogen-bonding network involving the ammonium and sulfate ions. It is therefore anticipated that cooperative interactions between the complexes are relatively weak. The model developed to interpret the effect of temperature on deuterated ammonium copper sulfate hexahydrate is therefore based upon those used successfully to describe the behavior of the isolated Cu(H₂O)₆²⁺-ions in Cu²⁺ doped zinc(II) Tutton salts.^{8,9} The solid is assumed to behave as a set of individual complexes, each having two possible energy states, with the effect of the cooperative interactions being simply to modify the energy separation between these states for each complex. The average *g*-values and bond lengths in the lattice as a whole are determined using random statistics. The present paper describes the application of this model to the temperature dependence of the *g*-values and Cu–O bond lengths of (ND₄)₂[Cu(D₂O)₆](SO₄)₂, and the results are compared with those reported for cooperative Jahn–Teller interactions in other systems. Comparisons are also drawn with the equilibria

(26) Bersuker, I. B. *The Jahn–Teller Effect and Vibronic Interactions in Modern Chemistry*; Plenum: New York, 1984.

(27) Reinen, D.; Atanasov, M. *Magn. Reson. Rev.* **1991**, *15*, 167.

(28) Reinen, D.; Friebel, C. *Struct. Bonding (Berlin)* **1979**, *37*, 1 and references therein.

(29) Maaskant, W. J. A. *Struct. Bonding (Berlin)* **1995**, *83*, 55.

(30) Ogihara, T. *J. Phys. Soc. Jpn.* **1995**, *64*, 4221.

(31) Wojtowicz, P. *J. Phys. Rev.* **1959**, *116*, 32.

Table 1. Crystallographical Data of $(\text{ND}_4)_2[\text{Cu}(\text{D}_2\text{O})_6](\text{SO}_4)_2$ at Various Temperatures

	<i>T</i> (K)					
	100	180	240	270	298	321
formula	$\text{D}_{20}\text{CuN}_2\text{O}_{14}\text{S}_2$					
fw	419.8					
space group	$P2_1/a$ (monoclinic)					
cryst size, mm	sphere, $r = 0.35$ mm					
<i>a</i> (Å)	9.392(2)	9.386(1)	9.369(8)	9.341(5)	9.297(5)	9.2696(4)
<i>b</i> (Å)	12.6698(8)	12.6611(5)	12.6201(8)	12.5745(6)	12.5119(6)	12.4780(7)
<i>c</i> (Å)	6.0680(8)	6.0871(5)	6.120(2)	6.150(1)	6.194(1)	6.2300(4)
β (deg)	107.14(2)	107.03(1)	106.78(4)	106.57(3)	106.36(3)	106.265(4)
<i>V</i> (Å ³)	690.0(2)	691.7(1)	692.8(5)	692.4(4)	691.3(4)	691.76(7)
<i>Z</i>	2					
D_{calc} (g cm ⁻³)	2.02					
μ (cm ⁻¹)	19.5					
diffractometer	Enraf-Nonius CAD4-MACH					
radiation	Mo K α					
DOMA ^a	0.59	0.58	0.53	0.49	0.55	0.63
DOMB ^a	0.97	0.70	0.46	0.46	0.45	1.08
APTA ^b	1.46	1.63	1.64	1.51	1.70	1.46
APTB ^b	1.90	1.07	0.33	0.35	0.33	2.21
NPIPRE ^c	1					
SIGMA ^c	0.030					
SIGPRE ^c	2.0					
MAXTIME ^c	40					
REPTIME ^d	5000	5000	5000	5000	5000	2800
2θ scan range (deg)	4–59	4–60	4–59	4–60	4–60	4–56
transmission factors	0.86–1.00	0.86–1.00	0.86–1.00	0.89–1.00	0.84–1.00	0.94–1.00
no. of unique nonspace group extinguished reflcns	1906	2001	1910	1997	1997	1613
no. of reflcns (<i>n</i>) used in least-squares with $I > 3\sigma_I$	1706	1769	1703	1739	1722	1267
no. of parameters (<i>p</i>) used in least-squares	118					
largest shift/error	0.03	0.01	0.00	0.01	0.00	0.00
R^e	0.029	0.028	0.028	0.030	0.035	0.032
R_w^f	0.042	0.038	0.040	0.042	0.052	0.037
goodness-of-fit ^g	2.12	2.02	2.31	2.35	3.04	2.12
largest peak in final ΔF map, e/Å ³	0.5	0.4	0.3	0.3	0.4	0.5

^a Omega scan width (deg) = DOMA + DOMB tan θ . ^b Detector aperture = APTA + APTB tan θ (mm, horizontal). ^c All intensities prescanned at a rate of 16.18° min⁻¹ (NPIPRE = 1); those obeying the prescan acceptance limit (SIGMA) of $(\sigma_I/I)_{\text{pre}} < 0.03$ were considered observed and not rescanned, while those obeying the prescan rejection limit (SIGPRE) of $(\sigma_I/I)_{\text{pre}} > 2.0$ were considered unobserved and also not rescanned. All others were rescanned by using variable rates so that the maximum scan times (MAXTIME) would not exceed 40s. ^d Standard reflections measured every REPTIME seconds. ^e $R = \sum ||F_o| - |F_c|| / \sum |F_o|$. ^f $R_w = [\sum w(|F_o| - |F_c|)^2 / \sum w|F_o|^2]^{1/2}$, where $w(\text{weight}) = [\sigma(F_o)]^{-2}$. ^g $S = [\sum w(|F_o| - |F_c|)^2 / (n - p)]^{1/2}$.

observed between the spin states of iron(II) complexes, as these have some features in common with the present system.³²

Experimental Section

Preparation of Compounds. The preparation of $(\text{ND}_4)_2[\text{Cu}(\text{D}_2\text{O})_6](\text{SO}_4)_2$ has been described previously.²³ A sample of $(\text{ND}_4)_2[\text{Zn}(\text{D}_2\text{O})_6](\text{SO}_4)_2$ was prepared by a similar method, and this was doped with a little Cu^{2+} by recrystallizing a mixture of the zinc(II) salt with a 2% mole equivalent of the copper(II) compound in D_2O . Analysis of the water evaporated from the compounds by mass spectroscopy indicated that $> \sim 96\%$ of the hydrogens had been replaced by deuterium atoms.

EPR Measurements. EPR spectra in the temperature range 77–340 K were measured using a JEOL JES-FE spectrometer operating at a Q-band frequency of ~ 34 GHz. The temperature was controlled and measured using a standard JEOL cryostat accessory. In the temperature range 4–77 K, spectra were recorded on a Varian E-15 spectrometer at X-band frequency (~ 9 GHz). The temperature was controlled and measured using an Oxford Instruments flow cryostat.

X-ray Measurements. The X-ray crystallographic studies were done using an Enraf-Nonius CAD4 MACH diffractometer with graphite monochromatic Mo K α radiation ($\lambda = 0.71073$ Å). A Crystal Logic liquid nitrogen cryostat was used to cool the crystal. To prevent loss of D_2O for the measurement at 321 K, the crystal was mounted in a quartz capillary containing a saturated solution of the compound in D_2O . Temperatures were measured using a Cole-Parmer digital

thermocouple probe. The unit cell constants and their standard deviations were determined by a least-squares treatment (CELDIM) of the angular coordinates of 25 high-angle 2θ reflections. The θ - 2θ scan mode was used with a variable scan rate. The intensities of three check reflections showed no discernible decrease. All diffraction intensities were corrected for Lorentz and polarization effects and for absorption using seven ψ scans. Previously determined atomic coordinates²² were used as the initial input. The structures were refined using full-matrix least-squares methods with anisotropic displacement factors for the non-H atoms and fixed isotropic *B*-values for the H's. Refinements were based on *F*, and computations were performed on a Dec-alpha computer using the teXsan software package. Unit cell parameters, data acquisition techniques, and structure refinement results are summarized in Table 1; Cu–O bond lengths and H-bond contacts are listed in Table 2. All atomic positions, bond lengths and angles, and hydrogen-bonding contacts are given in the Supporting Information.

Results and Discussion

Temperature Dependence of the Crystal Structure of $(\text{ND}_4)_2[\text{Cu}(\text{D}_2\text{O})_6](\text{SO}_4)_2$. The structure of $(\text{ND}_4)_2[\text{Cu}(\text{D}_2\text{O})_6](\text{SO}_4)_2$ is shown in Figure 1. The general packing of the centrosymmetric $\text{Cu}(\text{D}_2\text{O})_6^{2+}$ ions and the way in which the structure changes as a function of temperature is similar to that reported by Hathaway and Hewat²² and by Figgis et al.^{33,34} The most pronounced influence of temperature is the effect it has upon the Cu–O bond lengths. Neither the average value nor

(32) (a) König, E. *Struct. Bonding* **1991**, 76, 51. (b) Gütlich, P.; Hauser, A.; Spiering, H. *Angew. Chem., Int. Ed. Engl.* **1994**, 33, 2024.

Table 2. Copper–Oxygen Bond Lengths for $(\text{ND}_4)_2[\text{Cu}(\text{D}_2\text{O})_6](\text{SO}_4)_2$ at $(\text{NH}_4)_2[\text{Cu}(\text{H}_2\text{O})_6](\text{SO}_4)_2$ and Hydrogen-Bonding Distances at Various Temperatures

	T (K)							
	8 ^a	85 ^b	100	180	240	270	298	321
Cu–O Bond Lengths								
Cu(1)–O(7) ^c	2.009(1)	2.010(1)	2.008(3)	2.012(2)	2.022(2)	2.041(2)	2.078(3)	2.116(3)
Cu(1)–O(8) ^c	2.300(1)	2.301(1)	2.277(2)	2.273(2)	2.259(2)	2.244(2)	2.210(2)	2.181(3)
Cu(1)–O(9) ^c	1.961(1)	1.960(1)	2.298(2)	2.298(2)	2.284(2)	2.263(2)	2.222(3)	2.181(3)
			2.002(2)	2.008(2)	2.027(2)	2.041(2)	2.071(2)	1.950(3)
			1.958(2)	1.959(2)	1.959(2)	1.958(2)	1.960(2)	1.959(2)
			1.969(2)	1.966(2)	1.957(2)	1.958(2)	1.959(2)	
Hydrogen Bond Distances								
O(3) ⁱ ···D(12 ⁱ)			2.00(3)	2.02(3)	2.03(3)	2.03(4)	1.98(5)	2.08(4)
O(3) ⁱ ···D(12 ⁱⁱ)			2.09(3)	2.04(4)	2.01(4)	2.18(4)	2.23(3)	
O(3) ⁱ ···D(13 ⁱⁱⁱ)			2.74(3)	2.68(3)	2.61(3)	2.66(4)	2.51(5)	2.35(4)
O(3) ⁱ ···H(13 ⁱⁱⁱ)			1.89(3)	2.01(4)	2.12(4)	2.15(4)	2.09(3)	
O(3) ⁱ ···D(20 ⁱⁱ)			1.79(4)	1.80(3)	1.81(4)	1.79(4)	1.79(5)	1.98(4)
O(3) ⁱ ···H(20 ⁱⁱ)			1.96(4)	1.85(5)	1.97(5)	2.00(4)	1.92(3)	
O(4) ⁱ ···D(13 ⁱⁱⁱ)			2.02(4)	2.01(4)	2.05(4)	2.23(4)	2.28(5)	2.21(4)
O(4) ⁱ ···H(13 ⁱⁱⁱ)			2.52(3)	2.50(4)	2.50(4)	2.50(4)	2.45(3)	
O(4) ⁱ ···D(17 ^{iv})			2.02(4)	1.96(4)	1.98(4)	2.05(4)	1.83(5)	1.90(4)
O(4) ⁱ ···H(17 ^{iv})			1.92(4)	1.94(5)	1.76(4)	1.87(4)	1.86(3)	
O(5) ⁱ ···D(14 ^v)			1.99(3)	1.96(3)	1.98(3)	1.99(4)	2.08(5)	2.01(4)
O(5) ⁱ ···H(14 ^v)			1.91(4)	1.93(5)	1.93(5)	2.02(4)	2.00(3)	
O(5) ⁱ ···D(15 ^v)			1.95(4)	2.01(4)	2.04(4)	2.05(4)	2.11(5)	1.92(4)
O(5) ⁱ ···H(15 ^v)			2.09(4)	2.06(5)	1.95(4)	2.01(4)	2.11(3)	
O(5) ⁱ ···D(19 ^{vi})			1.97(4)	1.96(4)	1.96(4)	1.95(4)	1.95(5)	2.00(4)
O(5) ⁱ ···H(19 ^{vi})			1.92(4)	2.00(5)	2.12(4)	1.85(4)	1.86(3)	
O(6) ⁱ ···D(11 ^{vii})			2.00(4)	2.07(4)	2.15(4)	2.03(4)	1.96(5)	2.04(4)
O(6) ⁱ ···H(11 ^{vii})			2.15(4)	2.12(5)	2.01(4)	2.03(4)	2.04(3)	
O(6) ⁱ ···D(16 ^{viii})			1.98(4)	1.95(4)	1.90(4)	1.92(4)	1.93(5)	2.21(4)
O(6) ⁱ ···H(16 ^{viii})			2.14(3)	2.09(4)	2.20(4)	2.24(4)	2.00(3)	
O(6) ⁱ ···D(18 ^{vii})			2.07(4)	2.08(4)	2.13(4)	2.06(4)	2.10(5)	2.04(4)
O(6) ⁱ ···H(18 ^{vii})			1.91(4)	1.97(5)	2.07(4)	2.06(4)	2.06(3)	

^a Reference 33. ^b Reference 34. ^c Top line, Cu–O bond lengths for deuterated structure; bottom line, Cu–O bond lengths for hydrogenated structure (Simmons, Hitchman, Stratemeier, unpublished results). Symmetry code: (i) x, y, z ; (ii) $1/2 - x, 1/2 + y, 1 - z$; (iii) $1/2 + x, 1/2 - y, z$; (iv) $1 + x, y, 1 + z$; (v) $1/2 - x, 1/2 + y, 1 - z$; (vi) $-x, 1 - y, 1 - z$; (vii) $1/2 + x, 1/2 - y, 1 + z$; (viii) $x, y, 1 + z$.

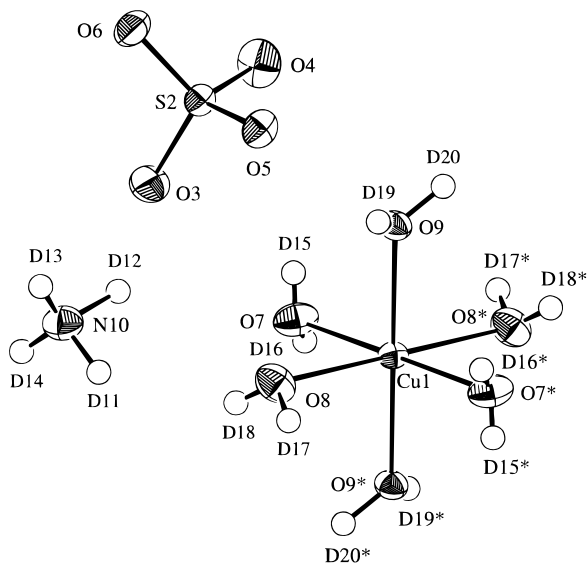


Figure 1. ORTEP drawing of the structure of $(\text{ND}_4)_2[\text{Cu}(\text{D}_2\text{O})_6](\text{SO}_4)_2$ at 298 K. Ellipsoids of 50% probability are shown. The $\text{Cu}(\text{D}_2\text{O})_6^{2+}$ ion is centrosymmetric.

the shortest Cu–O distance, that to O(9), changes as a function of temperature. The slight decrease in the Cu–O(9) bond length above ~ 250 K suggested by neutron powder data²² is not reproduced in the present, more accurate X-ray results. The other

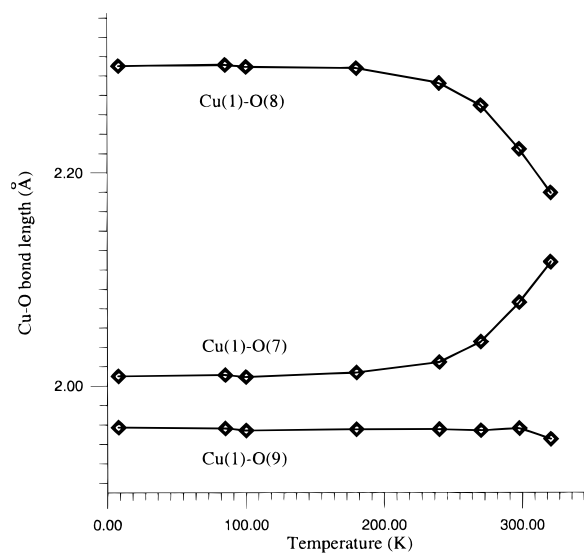


Figure 2. Plot of Cu–O bond lengths as a function of temperature for $(\text{ND}_4)_2[\text{Cu}(\text{D}_2\text{O})_6](\text{SO}_4)_2$. The convergence temperature of the Cu(1)–O(7) and Cu(1)–O(8) bond lengths, ca. 340 K, appears to correspond to the decomposition temperature of the crystal.

two Cu–O bond lengths remain nearly constant from ca. 15 to 180 K, but progressively converge above this temperature (see Figure 2).

The $\text{Cu}(\text{D}_2\text{O})_6^{2+}$ ions are interconnected by a hydrogen-bonding network, with the deuterium atoms of the water molecules forming hydrogen bonds with the sulfate ions, which in turn are linked by hydrogen bonds to the ammonia cations.

(33) Figgis, B. N.; Iverson, B. B.; Larsen, F. K.; Reynolds, P. A. *Acta Crystallogr.* **1993**, *B49*, 794.

(34) Figgis, B. N.; Khor, L.; Kucharski, E. S.; Reynolds, P. A. *Acta Crystallogr.* **1992**, *B48*, 144.

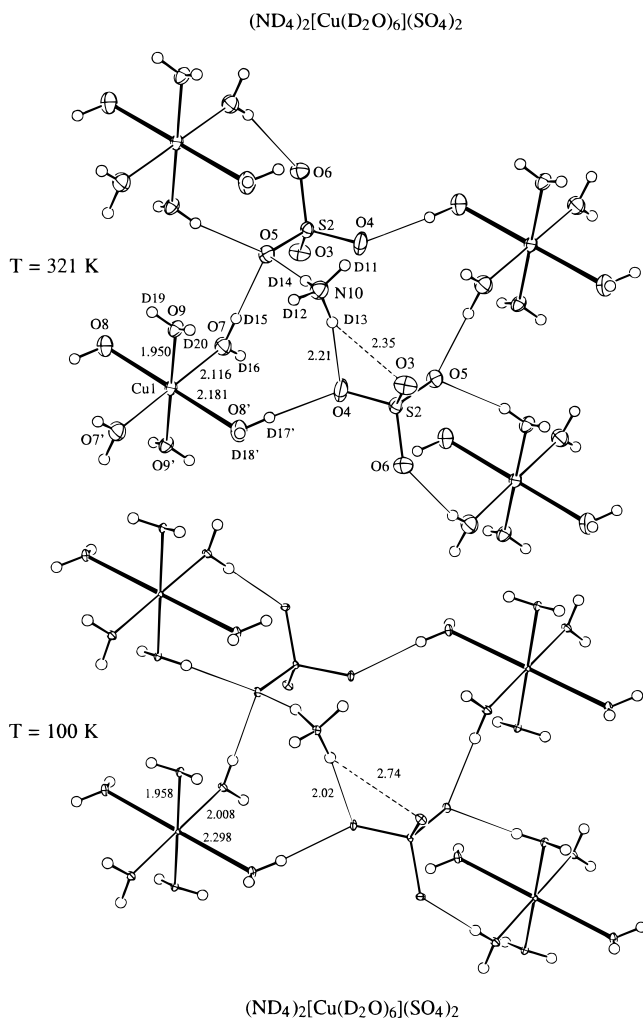


Figure 3. ORTEP drawing of part of the hydrogen-bonding network in $(\text{ND}_4)_2[\text{Cu}(\text{D}_2\text{O})_6](\text{SO}_4)_2$ at 321 and 100 K. Ellipsoids of 30% probability are shown. Cu–O and H–bond lengths are indicated in angstroms. Incipient H–bonds are indicated by dashed lines. Notice that the O(4)···D(13) and O(3)···D(13) contact distances are approaching each other at high temperatures.

The crystal packing is also influenced by temperature. Despite the changes in the Cu(1)–O(7) and Cu(1)–O(8) bond lengths, the hydrogen-bonding interactions, which are given in Table 2, do not change dramatically with temperature, except for O(4)···D(13), which increases from 2.02(4) Å at 100 K to 2.21(4) Å at 321 K (see Figure 3). This is because, above ca. 180 K, both the ammonium and sulfate groups undergo partial rotation, and this acts to minimize changes in most of the hydrogen-bonding contacts. In $(\text{NH}_4)_2[\text{Cu}(\text{H}_2\text{O})_6](\text{SO}_4)_2$, the O(3)···H(13) contact is stronger, varying from 1.89(3) Å at 100 K to 2.10(4) Å at 322 K, while the weaker O(4)···H(13) bond is 2.52(3) Å at 100 K and 2.15(4) Å at 322 K (see Figure 4).³⁵ Thus, these particular H bonds are converging to equal strengths in both structures with increasing temperature, an energetically unfavorable situation.

In considering the nature of the changes accompanying the rise in temperature, the structure of the corresponding hydrogenous salt is relevant. Here, the Cu(1)–O(7) and Cu(1)–O(8) bond lengths are reversed (Table 2), and the ammonium and sulfate groups have slightly different dispositions compared with the deuterated salt (see Figure 4).³⁵ In particular, the hydrogen

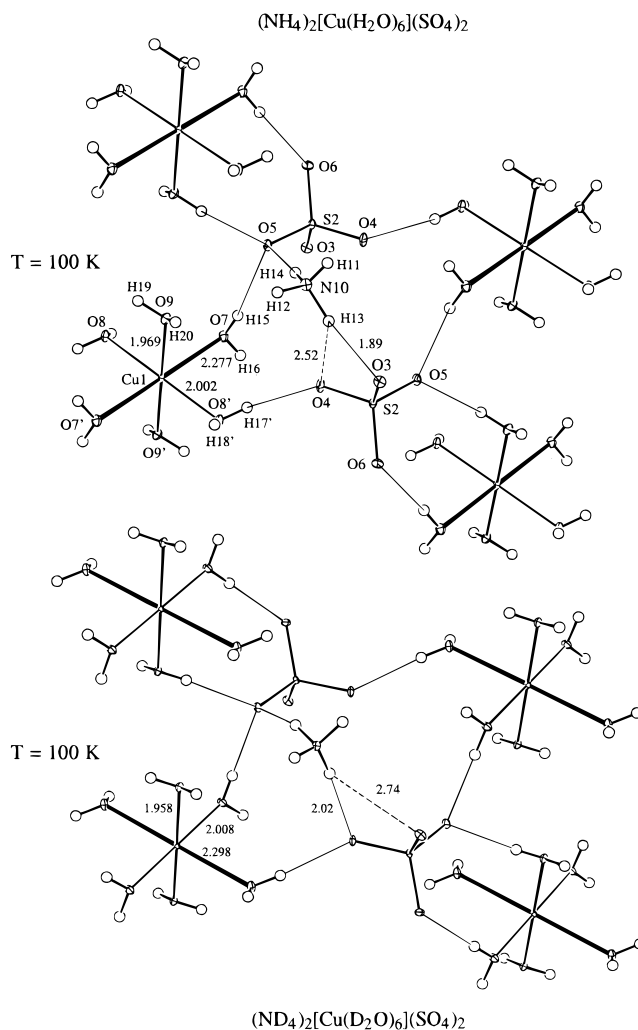


Figure 4. ORTEP drawing of part of the hydrogen-bonding network in the hydrogenated (top) and deuterated (bottom) ammonium copper Tutton salts at 100 K. Ellipsoids of 30% probability are shown. Cu–O and H–bond lengths are indicated in angstroms. Incipient H–bonds are indicated by dashed lines. Notice the switching of the Cu(1)–O(7) and Cu(1)–O(8) bond lengths.

bond between N(10) and sulfate O(3) is somewhat stronger, and that to O(4) somewhat weaker, in the hydrogenous compound (Table 2). The rotation of the ammonium and sulfate ions observed for $(\text{ND}_4)_2[\text{Cu}(\text{D}_2\text{O})_6](\text{SO}_4)_2$ as the temperature is raised carries these groups toward the dispositions observed for the hydrogenous salt, as shown in Figure 3. This suggests that the effect of temperature is to change the whole crystal structure toward that observed for the hydrogenous compound. On the basis of the structural data alone, it might be thought that the changes in the copper–oxygen bond lengths are due to the gradual onset of a phase transition due to a modification in which the $\text{Cu}(\text{D}_2\text{O})_6^{2+}$ ion exhibits a compressed tetragonal geometry, with this change being associated with the onset of the hindered rotation of the ND_4^+ groups. In fact, the EPR spectra are inconsistent with this interpretation (see following section), suggesting that the changes in the bond lengths are due to the presence of a thermal equilibrium with a higher energy form in which the geometry of the $\text{Cu}(\text{D}_2\text{O})_6^{2+}$ ion is similar to that observed at low temperature, but with the copper–oxygen distances to O(7) and O(8) reversed, as in the corresponding hydrogenous salt. The observed oxygen positions reflect the average of the positions of the two forms, weighted by their thermal populations. Similar structural equilibria have

(35) Simmons, C. J.; Hitchman, M. A.; Maaskant, W.; van der Plas, J.; Stratemeier, H. To be published.

been reported for a number of other copper(II) complexes.^{1,6} When disorder of this kind occurs, it is expected to produce an elongation of the thermal ellipsoid parameters along the directions of the bonds involved in the equilibrium, O(7) and O(8) in the present case. In favorable circumstances, analysis of the effect of temperature on the thermal parameters may yield information on equilibria of this kind.³⁶

As has been noted previously,²² the oxygen thermal ellipsoids for $(\text{ND}_4)_2[\text{Cu}(\text{D}_2\text{O})_6](\text{SO}_4)_2$ are not elongated appreciably along the bond directions, although there is still some evidence of disorder. For example, the mean-square vibrational amplitudes $\Delta U(\text{M}-\text{O})$ along the $\text{M}-\text{O}$ bonds for the deuterated ammonium copper and zinc Tuttons salts at 298 K are as follow: $\text{M}(1)-\text{O}(7) = 0.015, 0.002 \text{ \AA}^2$; $\text{M}(1)-\text{O}(8) = 0.011, 0.006 \text{ \AA}^2$; and $\text{M}(1)-\text{O}(9) = 0.005, 0.004 \text{ \AA}^2$ for $\text{M} = \text{Cu}$ and Zn , respectively. Although the ΔU values along the $\text{Cu}-\text{O}(7,8)$ bonds are considerably greater than those of the corresponding $\text{Zn}-\text{O}$ bonds, they are still somewhat smaller than those found for a typical Cu^{2+} pseudo-Jahn–Teller complex. For example, the $\text{Cu}-\text{O}$ bonds in the pseudo-Jahn–Teller complex $[\text{Cu}(\text{bipyam})_2(\text{ONO})]\text{NO}_2$ at 298 K are both $2.215(5) \text{ \AA}$,⁶ nearly the same as the $\text{Cu}(1)-\text{O}(8)$ bond in the deuterated ammonium copper Tutton salt. However, the $\Delta U(\text{Cu}-\text{O})$ value is 0.069 \AA^2 for the former versus 0.011 \AA^2 for the latter.³⁷ It may be that the reduction of the vibrational amplitudes along the bonds in the copper Tutton salts is partially the result of the hydrogen bonds between the water ligands and the sulfate O atoms, which are absent in the aforementioned pseudo-Jahn–Teller complex. The thermal parameters also show no apparent elongation along the $\text{Cr}-\text{O}$ bond axes³⁸ in the compound $[\text{Cr}(\text{H}_2\text{O})_6]\text{SiF}_6$, which contains tetragonally elongated octahedral $\text{Cr}(\text{H}_2\text{O})_6^{2+}$ ions with the distortion disordered over all three $\text{Cr}-\text{O}$ bond axes.³⁹

Temperature Dependence of the EPR Spectrum of $(\text{ND}_4)_2[\text{Cu}(\text{D}_2\text{O})_6](\text{SO}_4)_2$. Previous studies have shown^{7,9,19} that when Cu^{2+} is doped into a zinc(II) Tutton salt, the temperature dependence of the EPR spectrum of the resulting $\text{Cu}(\text{H}_2\text{O})_6^{2+}$ ion may be interpreted satisfactorily in terms of the behavior of an isolated complex. To provide a comparison to highlight the influence of cooperative effects in the pure copper(II) compound, the spectrum of $\sim 2\%$ Cu^{2+} doped into $(\text{ND}_4)_2[\text{Zn}(\text{D}_2\text{O})_6](\text{SO}_4)_2$ was therefore measured. The variation of the g -values (between 4 and 300 K) is shown in Figure 5. The g -values, and the way in which these change with temperature, are very similar to those reported previously by Riley et al.⁹ for $\sim 2\%$ Cu^{2+} doped into the corresponding hydrogenous zinc(II) compound, and the model applied to this system, referred to hereafter as the RWH model,⁹ was also used to interpret the present data. In this, the effects of Jahn–Teller coupling are applied to second order, with the resulting warped Mexican hat potential surface of the complex being perturbed by an orthorhombic lattice strain induced by the surrounding crystal lattice. The parameters used to define the warped Mexican hat potential surface and strain parameters giving optimum agreement with experiment were identical to those estimated⁹ for Cu^{2+} -doped $(\text{NH}_4)_2[\text{Zn}(\text{H}_2\text{O})_6](\text{SO}_4)_2$:

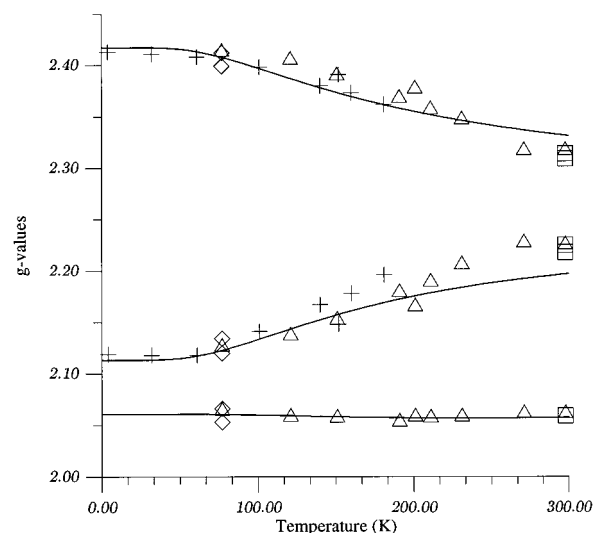


Figure 5. Temperature dependence of the g -values of $\sim 2\%$ Cu^{2+} doped into $(\text{ND}_4)_2[\text{Zn}(\text{D}_2\text{O})_6](\text{SO}_4)_2$. The crosses are derived from X-band measurements on a single-crystal oriented with the magnetic field close to the $\text{Cu}(1)-\text{O}(8)$ bonds of one complex and the $\text{Cu}(1)-\text{O}(9)$ bonds of the second molecule in the unit cell; the other symbols are from Q-band measurements on a powdered sample. The lines show the values calculated using the model of dynamic vibronic coupling described in ref 9; see text for the parameters used in the calculation and eq 1 and 2 for the definitions of the parameters and orientation of the g -axes.

$$A_1 = 900 \text{ cm}^{-1}$$

$$\bar{\nu} = 300 \text{ cm}^{-1}$$

$$A_2 = 33 \text{ cm}^{-1} \text{ (equivalent to a warping parameter)} \quad (1)$$

$$\beta = 300 \text{ cm}^{-1}$$

$$Q_q = -550 \text{ cm}^{-1}$$

$$Q_e = 120 \text{ cm}^{-1}$$

Here, A_1 is the first-order Jahn–Teller coupling constant, $\bar{\nu}$ the harmonic energy of the e_g vibration, A_2 is the second-order Jahn–Teller coupling constant, and Q_q and Q_e are the tetragonal and orthorhombic components of the lattice strain.

This implies that deuteration has little effect on the lattice of $(\text{NH}_4)_2[\text{Zn}(\text{H}_2\text{O})_6](\text{SO}_4)_2$. The change in structure which occurs upon deuteration of $(\text{NH}_4)_2[\text{Cu}(\text{H}_2\text{O})_6](\text{SO}_4)_2$ must, therefore, be due to a shift in what is a very delicate balance between the Jahn–Teller distortion of the metal complex and the hydrogen-bonding interactions in the lattice. The g -values of Cu^{2+} -doped $(\text{ND}_4)_2[\text{Zn}(\text{D}_2\text{O})_6](\text{SO}_4)_2$ do exhibit minor deviations from the behavior predicted by the RWH model in the higher temperature region (Figure 5). These could be due to residual cooperative interactions, or a slight variation of the lattice strain parameters with temperature. We are currently investigating these possibilities in conjunction with a detailed comparison of the effect of deuteration upon the crystal structure of the zinc(II) Tutton salt.

The potential surface of the $\text{Cu}(\text{D}_2\text{O})_6^{2+}$ ion in Cu^{2+} -doped $(\text{ND}_4)_2[\text{Zn}(\text{D}_2\text{O})_6](\text{SO}_4)_2$ is thus similar to that described previously⁹ for the corresponding hydrogenous complex. The warped Mexican hat potential surface has three minima, and the temperature dependence of the g -values is due to the change in the population of the two lowest vibronic levels, which are essentially localized in the two lower energy minima. The third minimum is too high in energy to be thermally populated at

(36) Bürgi, H.-B. *Trans. Am. Crystallogr. Assoc.* **1984**, *20*, 61. Stebler, M.; Bürgi, H.-B. *J. Am. Chem. Soc.* **1987**, *109*, 1395.

(37) Simmons, C. J. Unpublished results.

(38) Cotton, F. A.; Falvello, L. R.; Murillo, C. A.; Quesada, J. F. *J. Solid State Chem.* **1992**, *96*, 192.

(39) Falvello, L. R. *J. Chem. Soc., Dalton Trans.* **1997**, 4463–4475.

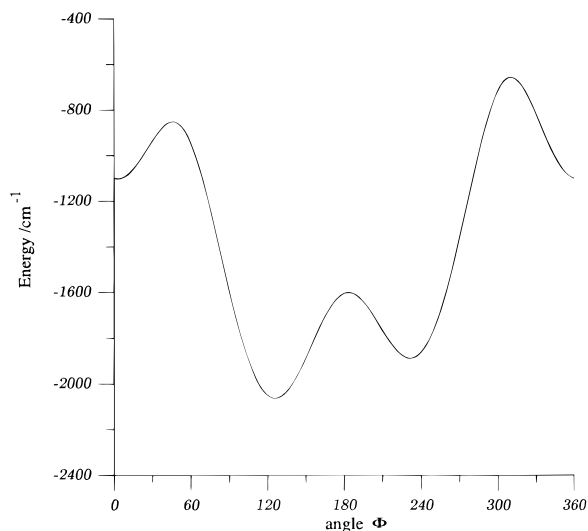


Figure 6. Variation of the energy minimum of the warped Mexican hat potential surface of the $\text{Cu}(\text{D}_2\text{O})_6^{2+}$ ion in Cu^{2+} doped into $(\text{ND}_4)_2[\text{Zn}(\text{D}_2\text{O})_6](\text{SO}_4)_2$, plotted as a function of the relative displacements of the two components of the Jahn–Teller vibration. The plot is only approximate, being measured at the radius of the Jahn–Teller minimum. The potential surface is identical to that calculated previously for Cu^{2+} doped into the corresponding hydrogenous zinc(II) salt; see ref 9.

the temperatures under consideration. A plot illustrating the warping of the Mexican hat potential surface is shown in Figure 6. The meaning of the plot has been discussed in detail previously.⁹ To a good approximation, the second vibronic level involves a wave function for which two of the g -values and concomitant bond lengths are interchanged compared with those in the ground level. With the direction of the axial and orthorhombic lattice strains defining the z and x axes, respectively, and a negative sign corresponding to a compression, the g -values of the first two levels are as follows:

$$\begin{aligned} \text{Level 1: } & g_x = 2.43, \quad g_y = 2.12, \quad g_z = 2.07 \\ \text{Level 2: } & g_x = 2.13, \quad g_y = 2.42, \quad g_z = 2.06 \quad (2) \end{aligned}$$

where x , y , and z are parallel to the $\text{Cu}-\text{O}(8)$, $-\text{O}(7)$, and $-\text{O}(9)$ bond directions, respectively. This suggests that, to a good approximation, the thermal behavior results from a Boltzmann equilibrium between structural isomers of the $\text{Cu}(\text{D}_2\text{O})_6^{2+}$ ion, these differing solely in the interchange of the bonds and electronic wave functions associated with the $\text{O}(7)$ and $\text{O}(8)$ water molecules. The two higher g -values change with temperature, as they represent the values weighted by the relative populations of the two vibronic levels, the rate of exchange between the levels being faster than the difference between their g -values expressed in frequency units. A model of this kind was first proposed by Silver and Getz⁷ to explain the temperature dependence of the EPR spectrum of Cu^{2+} doped into $\text{K}_2[\text{Zn}(\text{H}_2\text{O})_6](\text{SO}_4)_2$. This approach, subsequently referred to as the SG model, has been successfully used to interpret the temperature dependence of EPR spectra^{1,19} and $\text{Cu}-\text{O}$ bond lengths in a series of copper(II) compounds.⁶ The SG model implies that the ratio of the number of complexes in the lower level to that in the upper level, $K = n_1/n_2$, should obey the relationship $\ln K \propto 1/T$, where T is the absolute temperature. As may be seen from the plot shown in Figure 7a, the g -values of Cu^{2+} -doped $(\text{ND}_4)_2[\text{Zn}(\text{D}_2\text{O})_6](\text{SO}_4)_2$ obey this relationship reasonably well. As $K \propto e^{(E/kT)}$, where k is the Boltzmann constant, the slope of the line yields the energy difference between the two levels E . In the present case, the line of best fit yields the value

$E = 184 \text{ cm}^{-1}$, which agrees well with the difference between the two lowest vibronic levels estimated using the RWH model, 180 cm^{-1} , confirming that in this case the SG model is realistic.

In general terms, the variation as a function of temperature of the molecular g -values of the $\text{Cu}(\text{D}_2\text{O})_6^{2+}$ ion in pure $(\text{ND}_4)_2[\text{Cu}(\text{D}_2\text{O})_6](\text{SO}_4)_2$ is quite similar to that of Cu^{2+} -doped $(\text{ND}_4)_2[\text{Zn}(\text{D}_2\text{O})_6](\text{SO}_4)_2$. Typical powder spectra measured at Q-band frequency are shown in Figure 8. At low temperature, the EPR spectrum has near tetragonal symmetry, but as room temperature is approached the resonances due to the two higher g -values move together. The lowest g -value, g_z , does not change with temperature, and this shows that the actual local structure of the $\text{Cu}(\text{D}_2\text{O})_6^{2+}$ complex does not change from a tetragonally elongated toward a tetragonally compressed geometry, as might be inferred from the change in copper–oxygen bond distances (see preceding section). Such a structural change would require that the form of the ground-state wave function goes from $d_{x^2-y^2}$ toward d_z^2 . This would cause the lowest g -value to decrease significantly, as is, indeed, observed for complexes where the proportion of these orbitals in the ground-state varies as a function of temperature.^{4,11,40} This does not happen, and it may be inferred that the basic cause of the temperature dependence of the g -values of pure $(\text{ND}_4)_2[\text{Cu}(\text{D}_2\text{O})_6](\text{SO}_4)_2$ is similar to that in the doped complex. The potential surface of the $\text{Cu}(\text{D}_2\text{O})_6^{2+}$ ion is perturbed by lattice interactions. At low temperature, just the ground vibronic state is occupied, and the g -values reflect the true geometry of the complex. At temperatures above $\sim 200 \text{ K}$, a higher level, in which the g -values and bond lengths involving the $\text{O}(7)$ and $\text{O}(8)$ water molecules are reversed compared with the ground state, becomes thermally populated. As electron exchange between the levels is rapid on the EPR time scale, the g -values associated with these directions move progressively toward their mean value as the temperature is increased.

Although the basic cause of the thermal behavior of pure $(\text{ND}_4)_2[\text{Cu}(\text{D}_2\text{O})_6](\text{SO}_4)_2$ must be a thermal equilibrium of this kind, the way in which the g -values change with temperature cannot be interpreted satisfactorily using the models developed to describe the complexes formed when Cu^{2+} is doped into diamagnetic host lattices. A plot similar to that made for Cu^{2+} -doped $(\text{ND}_4)_2[\text{Zn}(\text{D}_2\text{O})_6](\text{SO}_4)_2$, based upon the SG model, which assumes that a Boltzmann distribution occurs between two energy states corresponding to different orientations of the $\text{Cu}(\text{D}_2\text{O})_6^{2+}$ ion, does not give a straight line (Figure 7b). A possible cause of the deviation might be that at high temperatures the rate of electron exchange between the two complexes in the unit cell becomes comparable to the EPR time scale, and this contributes to the partial averaging of the g -values. This cannot be the case, however, since a similar deviation is also observed in the variation of the bond lengths, and these are unaffected by the rate of electron exchange between the complexes. The most plausible explanation for the deviation is that the thermal equilibrium between two orientations of the complex does not obey Boltzmann statistics for the pure copper(II) compound. This seems reasonable because in the pure copper(II) compound, unlike the doped systems, when a complex at one lattice site is excited to a higher energy state, the change in geometry will influence the lattice strain acting upon its neighbors. Thus, in the pure compound, the average lattice strain acting on the $\text{Cu}(\text{D}_2\text{O})_6^{2+}$ ion is no longer independent of temperature, as assumed in the RWH and SG models. Because the complexes do not behave independently,

(40) Steffen, G.; Reinen, D.; Stratemeier, H.; Riley, M. J.; Hitchman, M. A.; Matthies, H. E.; Recker, K.; Wallrafen, F.; Niklas, J. R. *Inorg. Chem.* **1990**, *29*, 2123.

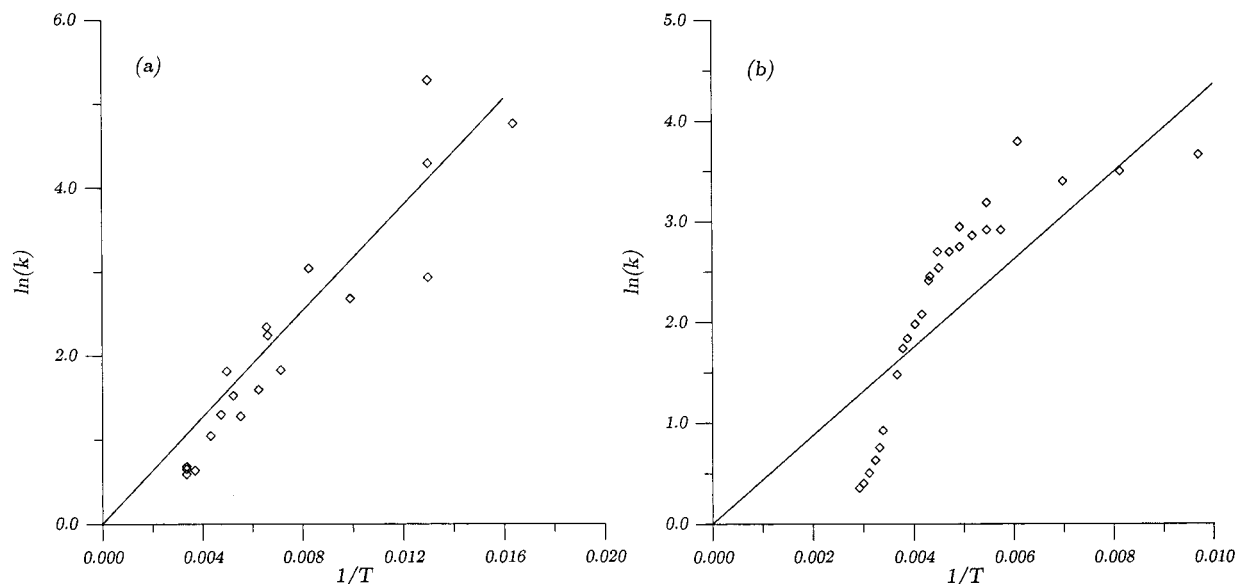


Figure 7. Plot showing the dependence of K , the ratio of complexes in the lower energy state to that in the upper state, and absolute temperature for (a) Cu^{2+} doped into $(\text{ND}_4)_2[\text{Zn}(\text{D}_2\text{O})_6](\text{SO}_4)_2$ and (b) pure $(\text{ND}_4)_2[\text{Cu}(\text{D}_2\text{O})_6](\text{SO}_4)_2$. The lines represent “best fits” assuming a linear relationship between $\ln K$ and $1/T$.

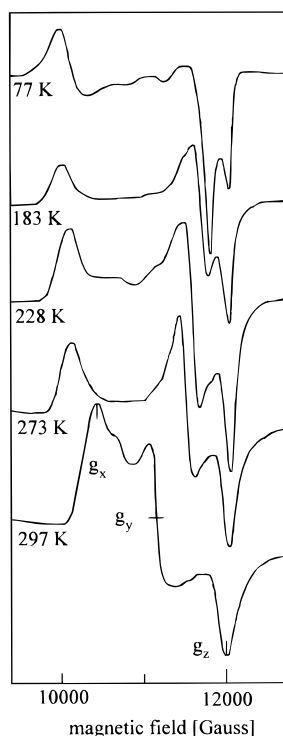


Figure 8. Typical EPR spectra of powdered $(\text{ND}_4)_2[\text{Cu}(\text{D}_2\text{O})_6](\text{SO}_4)_2$ at various temperatures measured at Q-band frequency.

cooperative interactions will influence the potential surfaces of the complexes and must be included in any model used to interpret their thermal behavior.

Cooperative Interactions in $(\text{ND}_4)_2[\text{Cu}(\text{D}_2\text{O})_6](\text{SO}_4)_2$. Within the framework of the SG model, the fact that a plot of $\ln K$ against $1/T$ is highly nonlinear for pure $(\text{ND}_4)_2[\text{Cu}(\text{D}_2\text{O})_6](\text{SO}_4)_2$ implies that the energy difference E between the two orientations of the $\text{Cu}(\text{D}_2\text{O})_6^{2+}$ ion varies as a function of temperature, and the sense of the curvature (Figure 7b) shows that E decreases as the temperature rises. A similar conclusion has been reached on the basis of the temperature dependence of the g -values of the corresponding hydrogenous compound.²¹ Similarly, the RWH model may be used to interpret the data for pure $(\text{ND}_4)_2$ -

$[\text{Cu}(\text{D}_2\text{O})_6](\text{SO}_4)_2$ if the energy separation between the two lower wells in the warped potential surface (Figure 6) is assumed to decrease progressively as the temperature increases—the g -value and bond length data may be reproduced satisfactorily if this separation approximately halves on going from 200 to 300 K. However, this conclusion applies to the lattice as a whole, whereas the calculations embodied in the RWH model,⁹ and indeed the SG model,⁷ refer to the potential surface of an isolated complex. Therefore, while it is true to say that the effect of the cooperative interactions is to make the energy difference between the two orientations of the $\text{Cu}(\text{D}_2\text{O})_6^{2+}$ ion temperature dependent, to interpret this quantitatively we need to consider how this occurs via modification of the potential surfaces of the individual complexes in the lattice. The problem is approached by considering that the energy of each complex is influenced by the orientations of its neighbors, with random statistics being used to determine the behavior of the population as a whole.

(a) Model Describing the Cooperative Interactions. For the reasons given above, it appears that the present problem involves just two states of the basic $\text{Cu}(\text{D}_2\text{O})_6^{2+}$ complex. Moreover, to a good approximation, the g -values and bond lengths of the upper state are very similar to those of the ground state, being simply interchanged in direction. At any temperature, the g -value and copper–oxygen distance associated with any particular bond are simply the average of those of the two states, weighted by the fraction of time the complexes spend in that state. At temperature T , this fraction of time is given by the expression

$$f = \exp(-E/kT) / [1 + \exp(-E/kT)] \quad (3)$$

where E is the energy of the upper state and k is Boltzmann’s constant. The cooperative interactions mean that, for pure $(\text{ND}_4)_2[\text{Cu}(\text{D}_2\text{O})_6](\text{SO}_4)_2$, the energy difference between the states of any particular complex depends on whether its neighbors are in the ground or upper state. In the present approach, the effect of the basic lattice strain, which is not influenced by the orientation of neighboring complexes or the temperature, is described by a parameter \mathbf{E} . Added to this is a contribution \mathbf{J} for each neighbor in “contact” with the particular

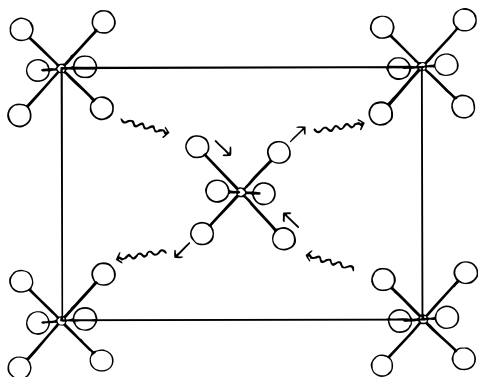


Figure 9. Schematic illustration of the cooperative interactions resulting from the thermal excitation of a $\text{Cu}(\text{D}_2\text{O})_6^{2+}$ ion in $(\text{ND}_4)_2[\text{Cu}(\text{D}_2\text{O})_6](\text{SO}_4)_2$.

complex under consideration. This depends on the relative orientation of the neighbor. For a complex in its ground state, the interaction is negative when a neighbor is also in its ground state, and the interaction is destabilizing and positive when it is in the upper state. As a starting point of the calculation, the lattice is assumed to have a particular distribution of complexes in the upper and lower states. The energy level separation of every complex is obtained in terms of \mathbf{E} and \mathbf{J} by noting the energy state of each neighbor. The Boltzmann equation (eq 3) is then applied to determine the probability that each complex is in its upper state. A random number generator is used to decide whether each complex is, in fact, in the upper or lower state. An iterative procedure is used to decide when the population of complexes has reached equilibrium after each temperature change. At convergence, the calculation yields the number of complexes in each state at any particular temperature, and hence the average Cu–O bond lengths and g -values.

Clearly, the approach depends on the symmetry relationships of the particular lattice under consideration. In general, the cooperative interactions may act differently along each Cartesian axis, and for a centrosymmetric octahedral complex three parameters \mathbf{J}_x , \mathbf{J}_y , and \mathbf{J}_z are required. In $(\text{ND}_4)_2[\text{Cu}(\text{D}_2\text{O})_6](\text{SO}_4)_2$, the $\text{Cu}(\text{D}_2\text{O})_6^{2+}$ ions stack in such a manner that the Cu–O bonds involved in the thermal equilibrium lie in a plane (see the next section and Figure 9). The cooperative interactions are therefore expected to involve a two-dimensional array with each complex in “contact” with four neighbors and $\mathbf{J}_z = 0$. Moreover, the long and intermediate bonds of neighboring complexes are approximately parallel. When one complex is thermally excited, it will act to “squeeze” two neighbors while applying a “negative pressure” to the other two, as illustrated schematically in Figure 9. To simplify the problem, we assume initially that these two effects are identical i.e., $\mathbf{J}_x = \mathbf{J}_y = \mathbf{J}$. At very low temperature, every complex in the lattice therefore has an energy $-4\mathbf{J}$, with an excited-state energy $\mathbf{E} + 4\mathbf{J}$. A complex with one neighbor in its excited state has an energy of $-2\mathbf{J}$ in the ground state and $\mathbf{E} + 2\mathbf{J}$ in the upper state. As the temperature rises, and more complexes go to the upper state, complexes with more than one neighbor in the upper state will occur, and the pattern of energy states develops further.

Based upon this model, a computer program was written to calculate the average g -values and Cu–O bond lengths in $(\text{ND}_4)_2[\text{Cu}(\text{D}_2\text{O})_6](\text{SO}_4)_2$ as a function of temperature. The physics of this problem are analogous to the Ising model for two-dimensional lattices.⁴¹ A numerical approach for simulating

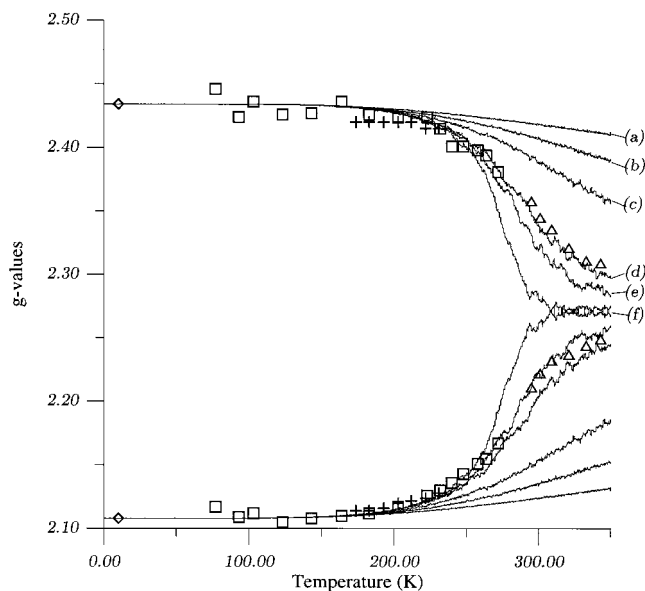


Figure 10. Temperature dependence of the g -values of $(\text{ND}_4)_2[\text{Cu}(\text{D}_2\text{O})_6](\text{SO}_4)_2$ estimated using various values of the basic lattice strain energy \mathbf{E} and cooperative interaction energy \mathbf{J} , both in cm^{-1} [(a) $\mathbf{E} = 621$, $\mathbf{J} = 0$; (b) $\mathbf{E} = 150$, $\mathbf{J} = 58.9$; (c) $\mathbf{E} = 50$, $\mathbf{J} = 71.4$; (d) $\mathbf{E} = 9$, $\mathbf{J} = 76.5$; (e) $\mathbf{E} = 5$, $\mathbf{J} = 77$; (f) $\mathbf{E} = 0$, $\mathbf{J} = 77.6$]. The best fit occurs for $\mathbf{E} = 9 \text{ cm}^{-1}$ and $\mathbf{J} = 76.5 \text{ cm}^{-1}$ (d). The symbols represent experimental measurements.

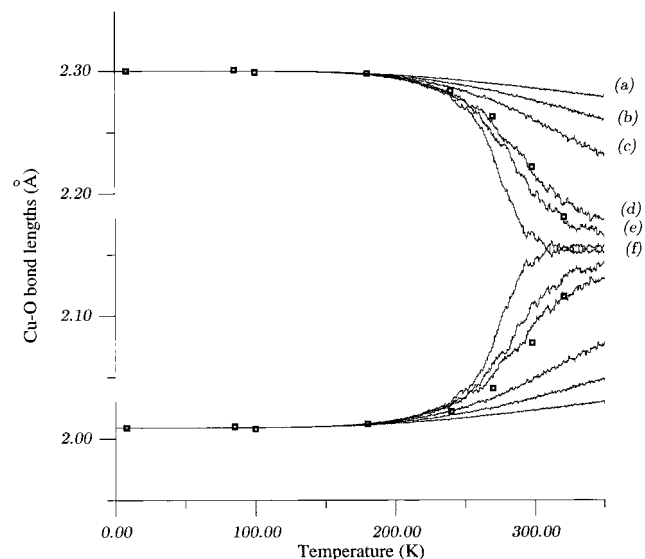


Figure 11. Temperature dependence of the Cu(1)–O(7) and Cu(1)–O(8) bond lengths of $(\text{ND}_4)_2[\text{Cu}(\text{D}_2\text{O})_6](\text{SO}_4)_2$ estimated using the values of the basic lattice strain energy \mathbf{E} and cooperative interaction energy \mathbf{J} as given in Figure 10. The best fit here also occurs for (d); the various symbols represent different experimental measurements.

cooperative Jahn–Teller effects in two dimensions has already been described.⁴² The temperature dependence of the population of complexes in the upper state, and hence the observed bond lengths and g -values, turns out to be quite sensitive to the values of \mathbf{E} and \mathbf{J} , as may be seen from the plots in Figures 10 and 11. Here, values of \mathbf{E} and \mathbf{J} have been chosen so that changes commence when the temperature rises to ~ 200 K. A lattice consisting of 180×180 complexes was used in the calculation, with periodic boundary conditions.⁴³ The “noise” in the curves

(42) Maaskant, W. J. A.; de Graaff, R. A. G. *J. Chem. Educ. B* **1986**, 63, 966.

(43) Born, M.; Huang, K. *Dynamical theory of crystal lattices*; Clarendon Press: Oxford, 1962.

(41) E.g.: ter Haar, D. *Elements of statistical mechanics*; Holt, Rinehart and Wilson: New York, 1961; Chapter 12.

reflects the fact that random statistics are used to generate the populations. The use of a smaller sized lattice simply increased this noise. Temperature steps of 1 K were used, with each data point being the average of four calculations. For each calculation, it was assumed that convergence had occurred when the change in population fraction was less than 0.003.

It is apparent that replacement of the basic lattice strain by a cooperative interaction causes the g -values and bond lengths to alter more rapidly as a function of temperature than is predicted by Boltzmann statistics. This is exactly what is observed when the behavior of pure $(\text{ND}_4)_2[\text{Cu}(\text{D}_2\text{O})_6](\text{SO}_4)_2$ is compared with that of Cu^{2+} -doped $(\text{ND}_4)_2[\text{Zn}(\text{D}_2\text{O})_6](\text{SO}_4)_2$. The temperature variation is quite sensitive to the ratio of the cooperative interaction to the basic lattice strain, and the behaviors of both the g -values and bond lengths of $(\text{ND}_4)_2[\text{Cu}(\text{D}_2\text{O})_6](\text{SO}_4)_2$ are reproduced satisfactorily using the same values for these, $\mathbf{E} = 9 \text{ cm}^{-1}$, $\mathbf{J} = 76.5 \text{ cm}^{-1}$, as may be seen from the data points shown in Figures 10 and 11. For Figure 10, the minor deviations at higher temperatures may be due to a slight increase in the average g -value associated with the “red-shift” of the excited-state energies which occurs on warming. Such an effect has been observed in other dynamic systems.¹² The fact that $\mathbf{J} \gg \mathbf{E}$ implies that the relative energies of the two lower wells of the warped Mexican hat potential surface of each $\text{Cu}(\text{D}_2\text{O})_6^{2+}$ ion are strongly influenced by the geometries of neighboring complexes, and that cooperative effects play a dominant part in the lattice interactions. The effect of removing the restriction $\mathbf{J}_x = \mathbf{J}_y$ was explored, and it was found that although this did not improve the fit with experiment, the data could be reproduced satisfactorily if one parameter is increased by up to $\sim 25\%$, while the other is reduced proportionately. If the anisotropy was further increased, agreement with experiment worsened progressively.

It seems reasonable that changing the geometry of one $\text{Cu}(\text{D}_2\text{O})_6^{2+}$ ion has a pronounced effect on the energies of its neighbors, since the bonds involved in the structural change lie in a plane in which the complexes are quite close to one another (Figure 9). The reason that the average energy difference between the two orientations decreases progressively as the temperature rises is that the potential surface, and hence the energy difference between the relevant vibronic energy levels of each complex, is influenced by the orientations of its neighbors. The lattice thus comprises an ensemble of complexes having a range of energy states. At low temperature, every complex is in a highly favorable environment, and the upper energy state has an energy $\mathbf{E} + 8\mathbf{J} \approx 620 \text{ cm}^{-1}$. When a complex is excited to this state, it destabilizes four neighbors, and the energy required to excite each of these decreases to $\mathbf{E} + 4\mathbf{J} \approx 315 \text{ cm}^{-1}$. If a complex has two neighbors in the excited state, a change in orientation does not alter the cooperative interaction, so only the small basic energy, $\mathbf{E} \approx 9 \text{ cm}^{-1}$, is required to cause excitation. As the temperature increases, and more and more complexes are thermally excited, the average energy required to populate the upper state thus decreases, as observed experimentally. It must be stressed that the numerical values presented here are not meant to be taken too literally—the model is very simplistic. For instance, next-nearest-neighbor interactions are ignored. However, the concept that at any instant of time the lattice comprises a set of complexes, each of which has energy levels which depend on the energy states of its neighbors, does appear to provide a useful description of the cooperative forces in the compound.

Because excitation of one complex enhances the probability that its neighbors will also undergo excitation, the model

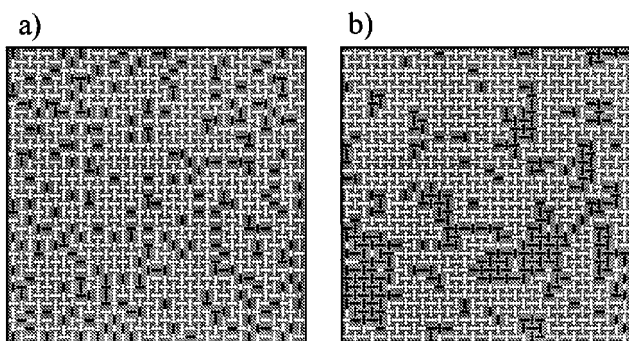


Figure 12. Schematic pictures of the orientations of the $\text{Cu}(\text{D}_2\text{O})_6^{2+}$ ions in $(\text{ND}_4)_2[\text{Cu}(\text{D}_2\text{O})_6](\text{SO}_4)_2$ estimated for a two-dimensional lattice of 35×35 complexes using the statistical model of cooperative Jahn–Teller coupling (a) with $\mathbf{E} = 200 \text{ cm}^{-1}$, $\mathbf{J} = 0 \text{ cm}^{-1}$ and (b) with $\mathbf{E} = 9 \text{ cm}^{-1}$, $\mathbf{J} = 76.5 \text{ cm}^{-1}$. For both pictures, $T = 280 \text{ K}$. The directions of the Cu–O long bonds of each complex are indicated by a dash, this being white when the complex is in its lower energy state and black when it is in its higher energy state.

suggests that the structural “switch” will not occur randomly throughout the lattice. The cooperative interactions should cause the excited complexes to tend to cluster in domains. To investigate this aspect, it is convenient to represent the disposition of the complexes visually. Pictures illustrating typical packing arrangements calculated with and without the influence of cooperative interactions are shown in Figure 12b and a, respectively. The direction of the long bond of the $\text{Cu}(\text{D}_2\text{O})_6^{2+}$ ion is illustrated by a dash, with this being white when it corresponds to the initial low-energy orientation and black when it corresponds to an excited high-energy orientation. Figure 12b shows a typical lattice at 280 K generated using the parameters giving optimum agreement with the data observed for $(\text{ND}_4)_2[\text{Cu}(\text{D}_2\text{O})_6](\text{SO}_4)_2$. Figure 12a illustrates the type of arrangement calculated for this lattice in the absence of cooperative interactions (i.e., assuming the SG model), with an energy separation between the orientations chosen to give a similar proportion of complexes in the higher energy state ($\sim 22\%$). In contrast to the random behavior exhibited by the complexes obeying simple Boltzmann statistics (Figure 12a), those in the lattice where strong cooperative interactions are present show a clear tendency for the excited complexes to aggregate with their bonds stacked in the stable antiferrodistortive manner (Figure 12b). This implies that many of the complexes which are thermally excited still have a packing arrangement similar to that in the ground state, but involving a set of complexes which have also switched their orientations. However, the position of the domains will fluctuate dynamically throughout the lattice. The partial averaging of the g -values and Cu–O bond lengths at high temperature may be understood as follows. For any particular complex, the length and associated g -value of each bond are the average of those of the two energy states weighted by the time the complex spends in that state. Consider a complex having a particular orientation at low temperature. On warming to 280 K, the complex spends $\sim 22\%$ of its time with the orientation reversed, probably as part of a domain in which the orientation is reversed for most complexes. The average atomic positions will therefore shift 22% of the way toward this new orientation, as will the g -values, provided that the complex exchanges between the energy levels more rapidly than the EPR time scale. The fact that the g -values are partially averaged at high temperature shows that this latter condition is satisfied.

In fact, some evidence that domains occur in crystals of $(\text{ND}_4)_2[\text{Cu}(\text{D}_2\text{O})_6](\text{SO}_4)_2$ at 12 K has already been provided from analysis of the line shapes observed for the diffraction

peaks from synchrotron-generated X-rays, though in this case these are thought to represent regions with somewhat different Jahn–Teller distortions at the Cu sites.⁴⁴ The ordering implied by domain formation should also affect the entropy of the system at high temperature, lowering this compared with a lattice having a similar number of complexes in the excited state, but distributed in a random fashion. This should influence the way in which the heat capacity of the compound varies with temperature. Complexes which exhibit equilibria between two spin states sometimes show thermal behavior which is quite similar to that exhibited by the present complex (see the section, Comparisons with Other Jahn–Teller Systems and High-Spin/Low-Spin Equilibria), and here evidence for the ordering of thermally excited complexes into domains under the influence of cooperative interactions has been obtained from differential calorimetry.⁴⁵ It is planned to undertake similar experiments on $(\text{ND}_4)_2[\text{Cu}(\text{D}_2\text{O})_6](\text{SO}_4)_2$. The behavior illustrated in Figure 12b is reminiscent of that which occurs for magnetic moments upon the breakup of magnetic ordering, and an attempt was made to look for the hysteresis effects commonly observed for magnetic materials. Hysteresis has, indeed, been observed for the structural change induced in $(\text{ND}_4)_2[\text{Cu}(\text{D}_2\text{O})_6](\text{SO}_4)_2$ by a variation in pressure.²⁵ However, the g -values were found to alter in the same way when the temperature decreased as when it increased, implying that no hysteresis occurs, at least over the time scale of these changes (a few minutes). A crystal was also cooled rapidly from room temperature to 4 K, but here also the spectrum was identical to that of a sample cooled slowly.

(b) Relationship between the Cooperative Interactions and the Crystal Structure. While the basic tetragonally elongated octahedral geometry of the $\text{Cu}(\text{D}_2\text{O})_6^{2+}$ ion is determined by the Jahn–Teller vibronic coupling, the modest orthorhombic distortion and the disposition of the complex are decided by interactions with the surrounding crystal lattice.⁴⁶ As discussed in detail previously,⁹ the lattice strain perturbs the warped Mexican hat ground-state potential surface, the main effect being to render the three minima inequivalent in energy to give a surface such as that shown in Figure 6. To a good approximation, each minimum corresponds to a similar geometry for the $\text{Cu}(\text{D}_2\text{O})_6^{2+}$ ion, but with the short, intermediate, and long Cu–O bond lengths (and associated electronic wave functions) occurring to different oxygen atoms. Considering the lattice interactions as constraints (i.e., as compressions), in $(\text{ND}_4)_2[\text{Cu}(\text{D}_2\text{O})_6](\text{SO}_4)_2$ the strongest interaction acts along the Cu(1)–O(9) direction, with a weaker interaction along Cu(1)–O(7) and the weakest interaction along Cu(1)–O(8). The lowest energy well of the potential surface therefore corresponds to a geometry with the short, intermediate, and long Cu–O bonds to these three oxygen atoms, respectively (Table 2). The well of intermediate energy, that which becomes thermally populated at room temperature, corresponds to a geometry in which the bonds to O(7) and O(8) are interchanged in length, while the highest well, which involves a lengthening of the bond to O(9), is not thermally populated at room temperature. The present model presumes that the cooperative interactions caused by the change in geometry of a complex act by influencing the lattice strain. It is therefore important to see whether the crystal packing

is consistent with this interpretation of the experimental observations.

The unit cell of $(\text{ND}_4)_2[\text{Cu}(\text{D}_2\text{O})_6](\text{SO}_4)_2$ has two $\text{Cu}(\text{D}_2\text{O})_6^{2+}$ ions in the unit cell. In the crystal plane in which the complexes are in closest contact, (001), one complex is located at the center of the unit cell, and this is linked via a hydrogen bond network to the four neighbors of the second type at the unit cell corners. The Cu(1)–O(7) and Cu(1)–O(8) bonds of both types of complexes lie approximately in this plane, with the bonds of intermediate length of the central complex, Cu(1)–O(7), being approximately parallel to the long bonds, Cu(1)–O(8), of two neighbors, and the long bonds of the central complex being nearly parallel to the intermediate bonds of the other two neighbors. Thus, the cooperative effects are expected to be dominated by interactions with four neighbors in a nearly two-dimensional array. When a complex is thermally excited, the lengthening of the Cu(1)–O(7) bonds will increase the strain acting along the Cu(1)–O(8) bonds of its two neighbors, while the concomitant shortening of the Cu(1)–O(8) bonds will reduce the compression acting on the Cu(1)–O(7) bonds of the other two neighbors (Figure 9). Both effects will reduce the orthorhombic component of the lattice strain, hence decreasing the energy difference between the two lower wells of the Mexican hat potential surface. This is just what is inferred from the behavior of the g -values and bond lengths. The axial component of the lattice strain, which influences the energy of the highest well, and which involves the wave function associated with a change in the Cu(1)–O(9) bond length and lowest g -value, should not be influenced by the cooperative interactions, and this also agrees with experiment. The packing of the complexes in the lattice is therefore exactly that expected to give the observed temperature dependence of the bond lengths and g -values.

If the present model is realistic, it implies that the influence of cooperative interactions on the g -values and bond lengths of complexes undergoing dynamic Jahn–Teller equilibria is closely related to the crystal packing of the complexes. The relatively simple behavior of the present compound, in which only the two higher g -values and the two longer bonds exhibit deviations from Boltzmann statistics, is due to the fact that here only the orthorhombic component of the lattice strain is affected by cooperative interactions. Such a situation is expected only for compounds in which the complexes pack with the long and intermediate bonds of neighboring complexes alternating and lying in one plane, the so-called antiferrodistortive arrangement. When this condition is not satisfied, a change in geometry of one complex may influence both the axial and orthorhombic components of the lattice strain of its neighbors. The cooperative interactions will then alter the warping of the potential surface in a manner that influences the temperature dependence of all three g -values and bond lengths. Such a situation occurs for the complex $\text{Cu}(\text{methoxyacetate})_2(\text{H}_2\text{O})_2$. Here, the temperature dependence of the g -values appears to obey simple Boltzmann statistics to a first approximation, but a detailed evaluation of the way the EPR spectra and crystal structure vary with temperature shows that, in fact, all *three* g -values and bond lengths show significant deviations from the behavior predicted by the SG model.⁴⁷ The crystal packing in this compound implies that a structural change in one complex is expected to influence the axial strain of its neighbors, and we are currently extending the present model in an attempt to treat this situation.

In considering the dynamic equilibrium, it is important to recognize that the structural change involves more than just the

(44) Figgis, B. N.; Reynolds, P. A.; Hanson, J. C.; Mutikainen, I. *Phys. Rev. B* **1993**, *48*, 13372.

(45) Jakobi, R.; Spiering, H.; Gmelin, E.; Güttlich, P. *Inorg. Chem.* **1988**, *27*, 1823 and references therein.

(46) For discussions of the way in which the balance between Jahn–Teller coupling and lattice interactions influence the geometry of a copper complex, see: Reinen, D.; Hitchman, M. A. *Z. Phys. Chem.* **1997**, *200*, 11.

(47) Jakob, B.; Reinen, D. *Z. Naturforsch.* **1987**, *42b*, 1500. Simmons, C. J.; Hitchman, M. A.; Stratemeier, H. Unpublished results.

copper complex. Partial rotations of the ammonium and sulfate ions also occur (see the section, Temperature Dependence of the Crystal Structure of $(\text{ND}_4)_2[\text{Cu}(\text{D}_2\text{O})_6](\text{SO}_4)_2$). Moreover, the water ligands are not in direct contact, so the cooperative interactions are, in fact, transmitted via a hydrogen-bonding network (see Figures 3 and 4). This network is presumably disrupted when one complex is thermally excited in isolation from its neighbors. The clustering of the excited complexes into ordered aggregates, as suggested by the present model, will minimize this disruption, which will occur only at the interface of the domains. The fact that cooperative interactions have a strong influence on the thermal equilibrium has implications for the interpretation of the structural change which occurs for $(\text{ND}_4)_2[\text{Cu}(\text{D}_2\text{O})_6](\text{SO}_4)_2$ at high pressure. Above ~ 300 bar, the structure alters to that of the corresponding hydrogenous compound, the most pronounced change being a “switch” in the Cu(1)–O(7) and Cu(1)–O(8) bond lengths analogous to that observed in the thermal equilibrium.^{23,24} In the mechanism proposed for this,²³ it was inferred that the lattice strain is pressure-dependent, changing in such a manner that the relative energies of the two lower wells in the warped Jahn–Teller potential surface are reversed in the high-pressure phase. Such a change might occur progressively, so that, in principle, it might be possible to fine-tune the pressure to produce a structure in which the two lower wells are equal in energy, so that the averaged bond lengths would correspond to a compressed tetragonal geometry. In practice, it does not seem possible to achieve this goal. Although the change has not yet been studied at the molecular level, the unit cell parameters do not change gradually from those of one phase to the other. Rather, they “switch” within a narrow pressure range, with no evidence for an intermediate phase.²⁵ The compound $(\text{NH}_4)_2[\text{Cr}(\text{H}_2\text{O})_6](\text{SO}_4)_2$ has a structure similar to that of $(\text{ND}_4)_2[\text{Cu}(\text{D}_2\text{O})_6](\text{SO}_4)_2$, and it has been observed⁴⁸ that doping the chromium compound with Zn^{2+} ions induces a structural change similar to that produced by pressure for the deuterated copper(II) salt. A switch in the structure of $(\text{ND}_4)_2[\text{Cu}(\text{D}_2\text{O})_6](\text{SO}_4)_2$ is also induced by doping with a small percentage (ca. 1.5%) of Zn^{2+} ions. Here, the switch appears to occur sharply, and it does not seem possible to produce an intermediate phase.⁴⁹ These results confirm that the structural changes cannot be thought of in terms of isolated copper complexes. Instead, a change in the geometry of one complex alters the hydrogen-bonding network, inducing a strong tendency for its neighbors, and indeed the lattice as a whole, to switch to the other structure. For the thermal equilibrium, this manifests itself in the formation of domains at high temperature, but for the changes induced by pressure or doping with Zn^{2+} ions, it has the effect of making the structure switch sharply from one phase to the other.

(c) Comparisons with Other Jahn–Teller Systems and High-Spin/Low-Spin Equilibria. As discussed already, the packing of the $\text{Cu}(\text{D}_2\text{O})_6^{2+}$ ions in $(\text{ND}_4)_2[\text{Cu}(\text{D}_2\text{O})_6](\text{SO}_4)_2$ corresponds to the antiferrodistortive arrangement of long and intermediate bonds observed for many six-coordinate Cu^{2+} complexes. The popularity of this type of structure is attributed to the fact that it optimizes the space requirements of the Jahn–Teller distorted complexes, and cooperative interactions are generally assumed to provide the basic driving force which causes the adoption of this type of lattice.²⁶ However, previous studies have usually focused on compounds where the complexes are in close proximity, as is the case in the hexanitro-

cuprates,²⁸ or on compounds where the metal ions are linked by bridging ligands. Here, large cooperative interactions are expected, since a change in the positions of the ligand atoms of one complex will have a strong influence upon the coordination geometry of its neighbors. The most pronounced effects occur in continuous lattices involving bridging ligands, as is the case, for instance, in K_2CuF_4 . This has planes of Cu^{2+} ions linked in an antiferrodistortive manner by bridging fluorides, with short terminal Cu–F bonds perpendicular to these sheets.⁵⁰ Here, an interchange in the bond lengths of the bridging fluorides at one atom must necessarily strongly perturb the coordination of its neighbors. Dynamic behavior of the kind observed for the Tutton salts is thus inhibited, and the structure of K_2CuF_4 is unchanged up to room temperature. When structural changes do occur on heating this type of compound, the cooperative interactions ensure that the atoms move in a concerted fashion, so that the phase changes are generally sharp, and to a new ordered structure. The effects of cooperative Jahn–Teller distortions and the way they are influenced by temperature in compounds of this kind may be rather complicated. For the compound CsCuCl_3 , where these interactions have been studied comprehensively, the vibrations of the whole unit cell, rather than just those of isolated complexes, must be included in the treatment in order to satisfactorily explain the structures observed at different temperatures.^{29,30} In these strongly coupled systems, the cooperative Jahn–Teller interactions are conventionally treated by means of parametrization schemes which refer to the whole ensemble of molecules in the lattice.^{26,31}

The structures of polynitocuprates of general formula $\text{A}_2\text{B}[\text{Cu}(\text{NO}_2)_6]$, where A and B represent a range of mono- and divalent cations, are also profoundly influenced by cooperative interactions. Here, the interactions between neighboring complexes are not cushioned by hydrogen-bonding effects, so the cooperative interactions are probably stronger than those in the Tutton salts, though considerably weaker than those in continuous lattices involving bridging ligands. In the γ phase of $\text{K}_2\text{Pb}[\text{Cu}(\text{NO}_2)_6]$, which is the stable form below 273 K, it is now known⁵¹ that the $\text{Cu}(\text{NO}_2)_6^{4-}$ ions have a tetragonally elongated octahedral geometry, with the long and one pair of short Cu–N bonds arranged in a two-dimensional antiferrodistortive packing arrangement (originally, the X-ray and EPR data were misinterpreted⁵² as indicating a ferrodistortive arrangement of tetragonally compressed octahedra). Above 280 K, a sharp phase transition to the α cubic phase occurs. Here, X-ray diffraction implies that each $\text{Cu}(\text{NO}_2)_6^{4-}$ ion has six identical Cu–N bond lengths, and the EPR signal is isotropic. However, it is thought that this is caused by a dynamic equilibrium in which the direction of the long bonds of each tetragonally elongated complex fluctuates randomly among the three Cartesian axes. Between 273 and 280 K, an intermediate β phase occurs, in which dynamic fluctuations of the long bonds occur, but only in the plane in which the long and short bonds are stacked in the low-temperature phase.⁵³ The behavior of $(\text{ND}_4)_2[\text{Cu}(\text{D}_2\text{O})_6](\text{SO}_4)_2$ thus shows similarities to that of $\text{K}_2\text{Pb}[\text{Cu}(\text{NO}_2)_6]$, the main difference being that the dynamic behavior increases gradually rather than sharply as the temperature is raised, without any change in the space group, and never reaches the stage that the dispositions of the long and short bonds become energetically equivalent. The relatively modest influence of the cooperative

(50) Hidaka, M.; Walker, P. J. *Solid State Commun.* **1979**, *31*, 383.

(51) Noda, Y.; Mori, M.; Yamada, Y. *Solid State Commun.* **1976**, *19*, 1071; **1977**, *23*, 24752.

(52) Harrowfield, B. V. *Solid State Commun.* **1976**, *19*, 983 and references therein.

(53) For a detailed discussion of the cooperative interactions in hexanitrocuprates(II), see ref 28, pps 26–40.

(48) Araya, M. A.; Cotton, F. A.; Daniels, L. M.; Falvello, L. R.; Murillo, C. A. *Inorg. Chem.* **1993**, *32*, 4853.

(49) Simmons, C. J.; Hitchman, M. A.; Stratemeier, H. Unpublished results.

interactions on the structural behavior of the Tutton salts presumably reflects the mediating influence of the hydrogen-bonding network.

The thermal behavior of $(\text{ND}_4)_2[\text{Cu}(\text{D}_2\text{O})_6](\text{SO}_4)_2$ is reminiscent of that of some of the complexes which exhibit equilibria between spin states. These also obey Boltzmann statistics in solution and when doped into the corresponding zinc compound, but they frequently show deviations attributed to cooperative interactions when in the pure state. Spin equilibria have been studied most comprehensively for Fe(II) compounds.³² Here, the structural changes range from sharp phase transitions involving a switch in space group, to more gradual changes in which the space group is maintained. Although the latter compounds are similar to $(\text{ND}_4)_2[\text{Cu}(\text{D}_2\text{O})_6](\text{SO}_4)_2$ as far as the underlying cause and basic pattern of behavior are concerned, there are important differences between the dynamic Jahn–Teller effect and spin equilibria. The latter involve two quite distinct electronic wave functions of a complex, whereas the former is usually best thought of as simply a change in orientation. Spin equilibria therefore involve forms which differ in entropy and other important properties, such as bond strength and light absorption. These complications are absent for most Jahn–Teller equilibria. For both kinds of equilibrium, the cooperative effects are due to the fact that thermal excitation of a complex causes a change in geometry, which may influence the energy states of its neighbors. However, a change from the high-spin ${}^5\text{T}_{2g}$ state of an octahedral Fe(II) complex to the low-spin ${}^1\text{A}_g$ state predominantly involves an approximately equal contraction in all the metal–ligand bonds—a displacement in the totally symmetric α_{1g} vibration. Although attempts have been made to develop a model in which Jahn–Teller distortions play an important role in the spin equilibria of iron(II) complexes,⁵⁴ it has been pointed out that the distortions are always very small and are not expected to influence the spin equilibria significantly.^{32b} The opposite is true for dynamic Jahn–Teller equilibria. Here, the two forms normally have similar average bond lengths, the energy difference simply involving a change in the orientation of the highly asymmetric complex in the crystal lattice. Because spin equilibria involve forms which differ significantly in volume, they are sensitive to changes in pressure. Jahn–Teller equilibria, on the other hand, involve a change in orientation of the asymmetric complex but almost no change in volume. In this context, it is interesting that $(\text{ND}_4)_2[\text{Cu}(\text{D}_2\text{O})_6](\text{SO}_4)_2$ in fact *does* show a switch in structure when subjected to pressure. However, it appears that this is due to the influence of pressure on the hydrogen-bonding interactions in the lattice, rather than on the geometry of the copper complex.⁴⁹

It is to be noted that, when the spin equilibria of complexes formed by doping are studied, the geometry of the guest complex is quite similar to that of the host. This has important consequences as far as the way in which cooperative interactions in spin equilibria are generally treated. The behavior of the complex at low concentration, where Boltzmann statistics are obeyed, is taken as the basic energy difference of the equilibrium. As the concentration of the guest Fe^{2+} complexes is progressively increased, additional cooperative interactions influence the thermal behavior, these reaching a maximum for the pure compound. The decrease in volume of the iron(II) complex which accompanies the ${}^5\text{T}_{2g} \rightarrow {}^1\text{A}_g$ spin change induces a negative pressure on its surroundings in the lattice. This causes the cooperative interaction which influences the energy difference between the spin “isomers”. Because the spin change alters the volume of the complex, and hence the crystal, the way in

which the unit cell dimensions respond to doping concentration and pressure provides useful information which may be incorporated into models describing the cooperative forces.^{32,55} It would be quite inappropriate to treat dynamic Jahn–Teller equilibria in a similar manner. When Cu^{2+} is doped into an analogous Zn^{2+} complex, the equilibrium refers to the change in orientation of a highly asymmetric complex in a lattice formed from essentially undistorted host complexes. This bears little correspondence to the corresponding energy difference in the lattice of the pure copper(II) compound, which is composed of highly distorted complexes. There is thus no reason the energy separation between the structural isomers of Cu^{2+} -doped $(\text{ND}_4)_2[\text{Zn}(\text{D}_2\text{O})_6](\text{SO}_4)_2$ should be similar to the basic energy difference of the forms involved in the thermal equilibrium of pure $(\text{ND}_4)_2[\text{Cu}(\text{D}_2\text{O})_6](\text{SO}_4)_2$. Similarly, the change in orientation involved in the Jahn–Teller equilibrium will not alter the crystal volume, so the overall compressibility of the crystal is not directly related to the mechanism by which the cooperative interactions are transmitted.

Conclusions

The temperature dependence of the two higher g -values of the $\text{Cu}(\text{D}_2\text{O})_6^{2+}$ ion formed when a small amount of Cu^{2+} is doped into $(\text{ND}_4)_2[\text{Zn}(\text{D}_2\text{O})_6](\text{SO}_4)_2$ may be interpreted satisfactorily using a simple model involving Boltzmann statistics, which assumes an equilibrium between structural isomers which differ solely in their orientation in the lattice. Basically similar behavior is observed for the g -values and two of the Cu–O bond lengths of pure $(\text{ND}_4)_2[\text{Cu}(\text{D}_2\text{O})_6](\text{SO}_4)_2$, except that as the temperature is raised these converge more rapidly than is predicted by Boltzmann statistics. It is presumed that the deviations from the simple model in the pure compound are due to cooperative interactions between the complexes—when one complex becomes thermally excited, it influences the energy states of its neighbors. The complexes are interconnected by hydrogen-bonding linkages which involve the ammonium and sulfate ions, and the changes in the Cu–O bond lengths which occur upon raising the temperature are accompanied by partial rotations of these two ions. The cooperative interactions are thus transmitted via a hydrogen-bonding network, and the thermal equilibrium involves the lattice as a whole, not merely the copper complexes. A model to describe the cooperative interactions is presented. This assumes each complex has two energy states which depend on its orientation in the lattice. However, the energy difference between the states of any particular complex depends on the orientation of its neighbors. The number of complexes in each energy state at any temperature is estimated using statistics. The statistical model explains the temperature dependence of the g -values and bond lengths of $(\text{ND}_4)_2[\text{Cu}(\text{D}_2\text{O})_6](\text{SO}_4)_2$ satisfactorily and suggests that the cooperative interactions have a dominant influence on the thermal behavior of the compound. A pictorial representation of the distribution of the complexes suggests that the cooperative interactions cause the thermally excited complexes to cluster in domains, and this explains several aspects of the behavior of $(\text{ND}_4)_2[\text{Cu}(\text{D}_2\text{O})_6](\text{SO}_4)_2$ under the influence of temperature and pressure. While the cooperative interactions in $(\text{ND}_4)_2[\text{Cu}(\text{D}_2\text{O})_6](\text{SO}_4)_2$ show some similarities to those in other copper(II) compounds, and to the spin equilibria exhibited by some iron(II) complexes,

(54) Kambara, T. *J. Phys. Soc. Jpn.* **1981**, *50*, 2257.

(55) Köhler, C. P.; Jakobi, R.; Meissner, E.; Wiehl, L.; Spiering, H.; Gütllich, P. *J. Phys. Chem. Solids* **1990**, *51*, 239.

important differences exist which necessitate the novel approach used to interpret these effects in the present compound.

Acknowledgment. M.A.H. is grateful to the Humboldt Foundation and the Australian Research Council for financial assistance. C.J.S. acknowledges a grant from the Polynesian Cultural Centre for the purchase of the Enraf Nonius CAD4-MACH diffractometer. Dr. H. Spiering of the Anorganische

Institut of the University of Mainz is thanked for useful discussions.

Supporting Information Available: Tables of atomic positions, bond lengths and angles, hydrogen-bonding contacts, and thermal parameters for $(\text{ND}_4)_2[\text{Cu}(\text{D}_2\text{O})_6](\text{SO}_4)_2$ (PDF). This material is available free of charge via the Internet at <http://pubs.acs.org>.

JA981831W